



TITLE:

# Bifurcations in resonantly forced water waves

AUTHOR(S):

Funakoshi, Mitsuaki; Inoue, Susumu

---

CITATION:

Funakoshi, Mitsuaki ...[et al]. Bifurcations in resonantly forced water waves. 数理解析研究所講究録 1991, 774: 126-138

ISSUE DATE:

1991-12

URL:

<http://hdl.handle.net/2433/82411>

RIGHT:

## Bifurcations in resonantly forced water waves

九大応力研 Mitsuki Funakoshi (船越満明)

九大応力研 Susumu Inoue (井上 進)

**Abstract.** Water waves are generated when a container halfly filled with a fluid is oscillated sinusoidally in a horizontal direction. For the resonant case in which a forcing period  $T$  is close to the natural period of two degenerate modes, Miles derived a nonlinear equation for four variables related to the modulations of these modes. We examine the  $T$ -dependence of solutions to this equation within the parametric region of no stable fixed point for several values of forcing amplitude  $x_0$  and damping coefficient  $\alpha$ . Based on the computations of periodic orbits (of period  $\tau$ ), we find that, when  $x_0$  increases with  $\alpha$  fixed or when  $\alpha$  decreases with  $x_0$  fixed, the  $T$ -dependence becomes more complicated owing to the generation of new branches of periodic orbit through homoclinic bifurcation, appearances of folds and kinks in the  $\tau$ - $T$  curve of each branch, merging of branches, and destabilization of periodic orbits by period-doubling and symmetry-breaking bifurcations.

### 1. Introduction

Water waves are generated when a cylindrical container filled with a fluid up to the depth  $d$  and of radius  $a$  is oscillated horizontally in one direction. The eigenmodes of these waves are generally written as  $\eta = (A_1(t) \cos m\theta + A_2(t) \sin m\theta) J_m(k_{m,n}r)$  for the free-surface displacement  $z = \eta$ . Here  $z$  is the vertical upward coordinate, and  $(r, \theta)$  plane polar coordinates on which the axis of oscillation is  $\theta = 0$  and  $\pi$ . Positive integer  $n$  is defined so that  $k_{m,n}a$  is the  $n$ -th positive zero of  $J'_m$ , while  $m$  is a circumferential wavenumber. In the  $(m, n)$  mode,  $A_1(t)$  and  $A_2(t)$  change sinusoidally with the natural frequency  $\omega_{m,n}$ .

We study the resonant case in which the displacement of the container is expressed as  $x = x_0 \cos(2\pi t/T)$  and the forcing period  $T$  is close to the natural period  $T_0 (= 2\pi/\omega_{1,1})$  of

two degenerate (1,1) modes. Here  $\omega_{1,1} = \sqrt{gk_{1,1} \tanh k_{1,1}d}$  ( $g$  : gravitational accerelation).

Then  $\eta$  can be approximately written as

$$\eta = a[(p_1 \cos \omega t + q_1 \sin \omega t) \cos \theta + (p_2 \cos \omega t + q_2 \sin \omega t) \sin \theta] J_1(kr). \quad (1)$$

Here  $\omega = 2\pi/T$ ,  $k = k_{1,1} = 1.8412/a$ , and four variables  $p_1$ ,  $q_1$ ,  $p_2$ , and  $q_2$  can change with the time scale much larger than  $T$ . In order to analyse this resonant case, [Miles, 1984] assumed that

$$\left. \begin{aligned} \varepsilon &\equiv (x_0/a)^{1/3} \ll 1, & p_n, q_n &= O(\varepsilon), & [n = 1, 2], \\ (\text{time scale of the changes of } p_n \text{ and } q_n)/T &= O(\varepsilon^{-2}), \\ T_r &\equiv (T - T_0)/T_0 = O(\varepsilon^2), \end{aligned} \right\} \quad (2)$$

and derived the following nonlinear equations for  $p_n$  and  $q_n$

$$\left\{ \begin{aligned} \dot{p}_1 &= -\alpha p_1 - (\beta + AE)q_1 + BMp_2, \\ \dot{q}_1 &= -\alpha q_1 + (\beta + AE)p_1 + BMq_2 + cx_0/a, \\ \dot{p}_2 &= -\alpha p_2 - (\beta + AE)q_2 - BMp_1, \\ \dot{q}_2 &= -\alpha q_2 + (\beta + AE)p_2 - BMq_1, \end{aligned} \right. \quad (3)$$

under the assumptions of weak nonlinearity and linear damping of  $O(\varepsilon^2)$ . Here dots denote the derivative with respect to  $t' (= \omega t)$ . Since  $M = p_1q_2 - p_2q_1$  and  $E = (p_1^2 + q_1^2 + p_2^2 + q_2^2)/2$ , the terms including  $M$  or  $E$  are nonlinear ones of third-order. The parameter  $\beta$ , given by  $\beta = (\omega^2 - \omega_{1,1}^2)/2\omega_{1,1}^2$ , corresponds to the difference between the natural frequency (period) and the forcing frequency (period). We hereafter use  $T_r$  defined in (2) in place of  $\beta$  to express this difference. Also  $\alpha$  is a coefficient of linear damping. The values of coefficients  $A$ ,  $B$ , and  $c$  depend only on  $a/d$ . [Miles, 1984] found that (3) has periodic and chaotic solutions as well as fixed points. In this paper, we examine the dependences of the solutions to (3) on parameters  $x_0/a$ ,  $\alpha$ , and  $T_r$  in detail. Here we used the values  $A = 0.224$ ,  $B = -0.306$ ,  $c = 1.315$ , which correspond to  $a/d = 0.655$ .

## 2. Solutions to equation (3)

Equation (3) has the property that if  $(p_1(t'), q_1(t'), p_2(t'), q_2(t'))$  is a solution to (3) for parameters  $\alpha$ ,  $x_0/a$ ,  $\beta$ ,  $A$ ,  $B$ , and  $c$ , then for any positive value  $\nu$ ,  $(\nu p_1(\nu^{-2}t'), \nu q_1(\nu^{-2}t'),$

$\nu p_2(\nu^{-2}t'), \nu q_2(\nu^{-2}t')$ ) is the solution for parameters  $\nu^2\alpha, \nu^3x_0/a, \nu^2\beta, A, B$ , and  $c$ . Therefore, we can obtain essentially the same solution for all sets of values of  $(x_0/a, \alpha)$  satisfying the condition  $\alpha/(x_0/a)^{2/3} = \text{const.}$  under the appropriate transform of the value of  $T_r$ . Therefore, we hereafter fix the value of  $\alpha$  to 0.0043 and examine the  $T_r$ -dependence of the solution for several  $x_0/a$ .

Fixed points of (3) are composed of a one-dimensional mode in which only  $\cos \theta$  mode is excited ( $p_2 = q_2 = 0$ ) and a rotational mode in which both  $\cos \theta$  and  $\sin \theta$  modes are excited and the point of largest  $\eta$  rotates in a definite direction [M, 1984]. Figure 1 shows a typical  $T_r$ -dependence of fixed points. Supercritical Hopf bifurcations (hereafter referred to as H.b.'s) of the rotational mode occurs at two points A and B. Since this mode is unstable between these points, there is no stable fixed point in the  $T_r$  region between A and C, a turning point of the one-dimensional mode. For sufficiently small  $x_0$ , however, since the H.b. does not occur, at least one stable fixed point exists for all  $T_r$ . These results are summarized in Fig.2, where no stable fixed point exists in a hatched region. We mainly examine the solutions for parameters in this region.

We first computed a series of attractors for a few fixed values of  $x_0$  by slowly increasing  $T_r$  from the value a little smaller than the left edge of the above parametric region. For each attractors, we computed the set  $S$  of values taken by  $M$  when the orbit intersects a hyperplane  $p_1 = \langle p_1 \rangle$ . Here  $\langle p_1 \rangle$  is the average value of  $p_1$ . For fairly small  $x_0$ , within wide regions of  $T_r$ ,  $S$  is composed of few points, corresponding to the limit cycles which express periodic modulations of water waves (see Fig.3(a)). And only in few relatively narrow regions of  $T_r$ , we find chaotic attractors in which  $S$  is composed of many points and which correspond to irregular modulations of water waves. For large  $x_0$ , however, chaotic attractors are found more commonly, and limit cycles exist in many narrow windows, as shown in Fig.3(b). The alternation between limit cycles and chaotic attractors is frequent for large  $x_0$ . Therefore, the  $T_r$ -dependence of the attractors becomes more complicated with the increase of  $x_0$ . Furthermore, we find the following variations of the  $T_r$ -dependence

of limit cycles caused by the increase of  $x_0$  : (i) A limit cycle revealing continuous  $T_r$ -dependence loses the continuity at a certain  $x_0$ . (ii) The  $T_r$  region where a limit cycle exists with the continuous  $T_r$ -dependence extends abruptly at a certain  $x_0$ .

### 3. Periodic orbits

Aiming at resolving the process to more complicated  $T_r$ -dependence of the attractors associated with the increase of  $x_0$ , we computed, as the first step, periodic orbits of (3) with a kind of Newton method, almost the same as those introduced in [Sparrow, 1982]. The periodic orbits are classified into a unidirectional periodic orbit (hereafter referred to as u.p.o.) and a bidirectional periodic orbit (b.p.o.). Here u.p.o., corresponding to the unidirectional rotation of the point of largest  $\eta$  of water waves, yields the  $M$  values of definite sign almost all time. On the contrary,  $M$  for b.p.o. takes both positive and negative values, expressing the alternations of clockwise and anticlockwise rotations of water waves. Furthermore, b.p.o. is composed of symmetric and asymmetric ones, only the former of which is invariant with respect to the transformation  $(p_1, q_1, p_2, q_2) \rightarrow (p_1, q_1, -p_2, -q_2)$ . We mainly examine the symmetric ones.

Stable fixed points exist for all  $T_r$  only if  $x_0$  is less than  $0.00103a$ , as shown in Fig.2. Period  $\tau$  of periodic orbits for  $x_0$  a little larger than this value is shown in Fig.4(a). We find an approximately straight branch of stable u.p.o. connecting  $H_1$  and  $H_2$ , the H.b. points of the rotational mode. With the increase of  $x_0$ , a part of large  $\tau$  appears on this branch, as shown in Fig.4(b), and then the separation of the u.p.o. branch associated with the appearance of a symmetric b.p.o. branch is found, as shown in Fig.4(c). Here and hereafter half the period is expressed for b.p.o.'s in figures. At the boundaries of these branches,  $\tau$  tends to infinity indicating the existence of homoclinic orbits associated with the fixed point of the one-dimensional mode. This kind of homoclinic bifurcation (hereafter referred to as h.b.) occurs also for larger  $x_0$ . In Fig.5, we can see five branches resulting from the separation of the b.p.o. branch in Fig.4(c) associated with the appearance of a new u.p.o. branch. These h.b.'s are summarized in Fig.6. Here solid lines denote the parameter values

for homoclinic orbits excepting that the lowest solid line is the H.b. point of the rotational mode. It can be roughly said that in each region surrounded by these lines, each u.p.o. or b.p.o. branch exists.

The behaviour of the  $\tau$ - $T_r$  curve when  $\tau$  tends to infinity is classified into two types. In type I,  $T_r$  increases or decreases monotonically as  $\tau \rightarrow \infty$ , while  $T_r$  oscillates with decreasing amplitude in type II. In Fig.6, crosses and circles denote type I and II, respectively. [Glendinning and Sparrow, 1984] examined a three-dimensional system containing a homoclinic orbit associated with a fixed point of saddle-focus type with eigenvalues  $\nu_1(> 0)$  and  $\nu_2 \pm i\omega_2$  ( $\nu_2 < 0$ ). According to a local analysis, they showed that type I and II are obtained when  $|\nu_2|/\nu_1$  is larger and smaller than one, respectively. The eigenvalues of the fixed point related to the homoclinic orbits in our four-dimensional system (3) have the same properties as the above eigenvalues except for the addition of the fourth one  $\nu_3(< 0)$ . The computed value of  $|\nu_2|/\nu_1$  in (3) is smaller than one in the region above the doubly-dotted broken line in Fig.6. Therefore, the types of the  $\tau$ - $T_r$  curve in (3) can be explained well based on the result of above analysis. This is probably because  $|\nu_3|/|\nu_2|$  is so large that the fourth dimension can be approximately neglected.

We call the u.p.o. branch starting from the lower H.b. point as branch I, and the next b.p.o. branch as branch II. We examine these branches in detail. The orbit in branch I is stable for all  $T_r$  if  $x_0$  is small enough not to undergo the h.b., as shown in Figs.4(a) and (b). At  $x_0$  close to the value of the first h.b., a fold of the  $\tau$ - $T_r$  curve of this branch appears, as shown in Fig.4(c), and discontinuous  $T_r$ -dependence of limit cycles and hysteresis are observed. For larger  $x_0$ , a stable region of this branch becomes unstable through a pair of supercritical period-doubling bifurcations (hereafter referred to as p.d.b.'s), as shown in Fig.7(a). The attractors in this destabilized region become more complicated through successive p.d.b.'s as  $T_r$  goes farther from the points of the first p.d.b. When the width of this region is sufficiently large, chaotic attractors appear at the central part of this region. One typical example is shown in the region  $0.0065 \leq T_r \leq 0.0095$  of Fig.3(a). Next at

$x_0 = 0.00224a$ , a new u.p.o. branch (referred to as branch  $I^+$ ) emerges as a small closed  $\tau$ - $T_r$  curve, whose size then becomes larger as  $x_0$  increases. Branches  $I$  and  $I^+$ , which are separated in Fig.7(b), merge at  $x_0 = 0.002294a$ , as shown in Fig.7(c). Consequently, when  $T_r$  is decreased from points A in Figs.7(b) and (c), the relevant limit cycle exists continuously only until  $T_r = 0.0102$  in (b), while until  $T_r = 0.0088$  in (c). That is, the  $T_r$  region where the limit cycle exists continuously extends abruptly owing to the merging of two branches. As  $x_0$  increases further, the  $\tau$ - $T_r$  curves in Figs.7 (d)-(f) reveal more complicated winding through the appearance of folds and the merging with other branches. For example, a new branch appeared at  $x_0 = 0.00344a$ , illustrated in Fig.7(e), merges with branch  $I$ , as shown in Fig.7(f). Moreover, the width of unstable regions emerged through p.d.b.'s becomes larger as  $x_0$  increases, resulting in the contraction of stable regions to narrow windows.

Periodic orbits in branch II are stable for all  $T_r$  just after its appearance through h.b. at  $x_0 = 0.001195a$ , as shown in Fig.4(c). Similarly to the case of branch  $I$ , a fold appears as  $x_0$  increases (see Fig.5). Moreover, a stable region of this branch becomes unstable through a pair of symmetry-breaking bifurcations (hereafter referred to as s.b.b.'s), as illustrated in Figs.5 and 8(a). Near the both ends of the destabilized region, asymmetric b.p.o.'s are obtained as attractors. Furthermore, successive p.d.b.'s of these b.p.o.'s and chaotic attractors are found when the width of this region is sufficiently large. If  $x_0$  increases further, a kink appears in a part of the  $\tau$ - $T_r$  curve, as found in Fig.8(c), resulting in discontinuous  $T_r$ -dependence and the occurrence of hysteresis of the limit cycle. At  $x_0 = 0.00244a$ , a new branch called as branch  $II^+$  emerges. Branches  $II$  and  $II^+$ , separated in Fig.8(c), merge at  $x_0 = 0.002483a$ , as found in Fig.8(d). (The intersection of the  $\tau$ - $T_r$  curves of these branches in Fig.8(c) does not mean the connection of them.) Therefore, the abrupt change of the  $T_r$  region where the limit cycles decreasing from B in Figs.8(c) and (d) exist continuously occurs. For larger  $x_0$ , further appearances of kinks and folds and occurrences of s.b.b.'s give rise to the state of many narrow windows of stable periodic orbits (see Figs.8(e) and (f)).

#### 4. Conclusions

Based on the computations of periodic orbits of (3) in the parametric region of no stable fixed point, we found that, when  $x_0$  increases with  $\alpha$  fixed, the  $T_r$ -dependence of the solutions to (3) becomes more complicated owing to the generation of new branches of periodic orbit through h.b., appearances of folds and kinks in the  $\tau$ - $T_r$  curve of each branch, merging of branches, and destabilization of periodic orbits by p.d.b.'s and s.b.b.'s. According to the property of (3) mentioned in section 2, this complication of the  $T_r$ -dependence occurs also when  $\alpha$  decreases with  $x_0$  fixed.

We acknowledge the technical assistance of Miss Hoshino.

#### REFERENCES

- Glendinning, P. and Sparrow, C., 1984, Local and Global Behavior near Homoclinic Orbits, *J. Stat. Phys.*, **35**, 645-696.
- Miles, J. W., 1984, Resonantly Forced Surface Waves in a Circular Cylinder, *J. Fluid Mech.*, **149**, 15-31.
- Sparrow, C., 1982, *The Lorenz Equations : Bifurcations, Chaos, and Strange Attractors*, Springer-Verlag, New York.



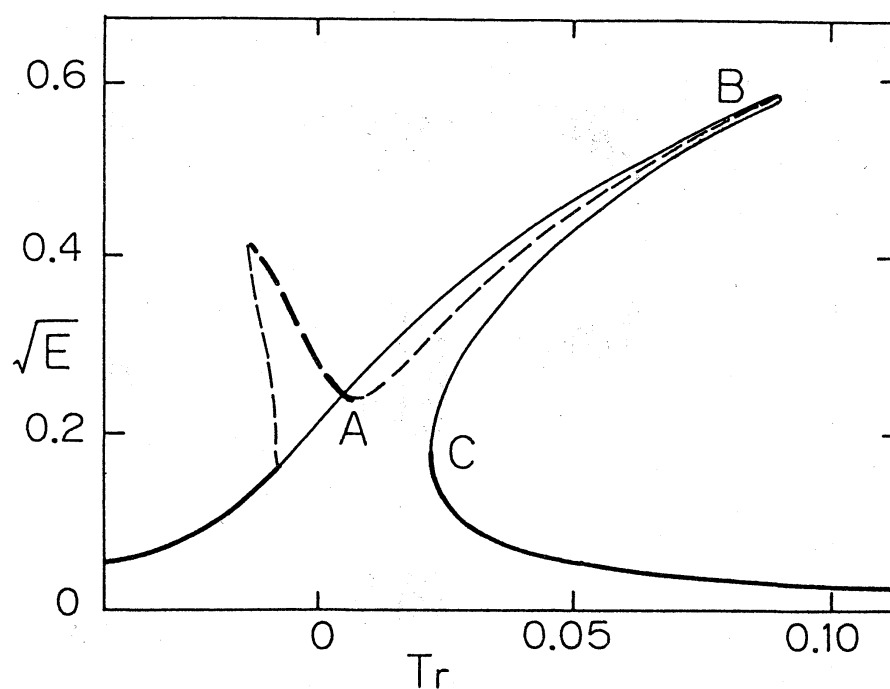


Fig.1 Typical  $T_r$ -dependence of fixed points. Solid line denotes the one-dimensional mode, and broken line the rotational mode. Bold and thin lines express stable and unstable fixed points, respectively.  $x_0=0.002706a$ .

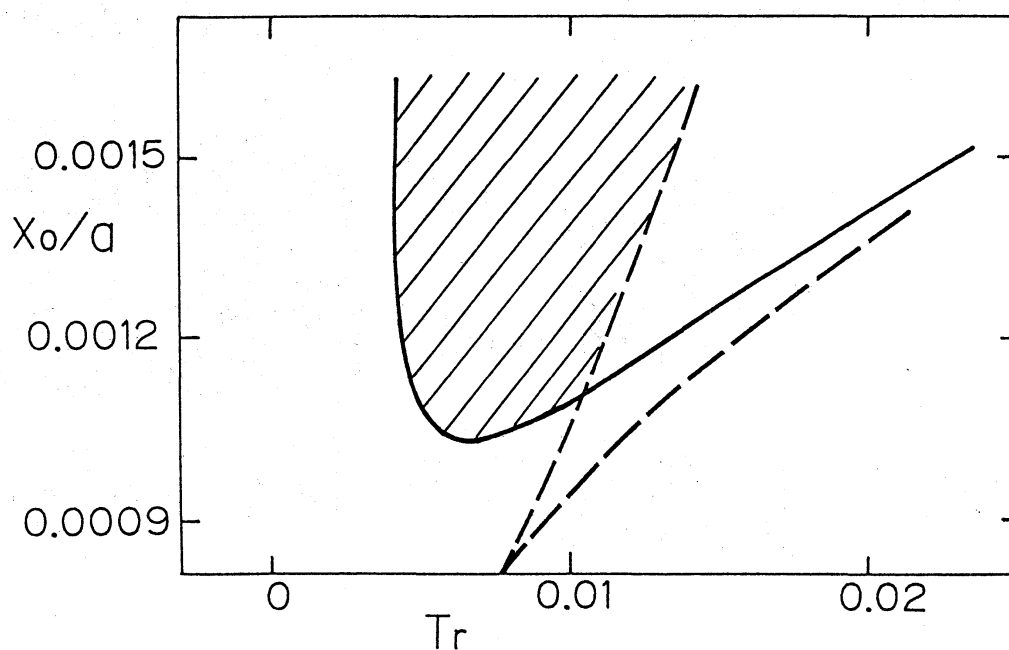


Fig.2 Bifurcation points of fixed point. Solid line denotes the H.b. point of the rotational mode, and broken line the turning point of the one-dimensional mode.

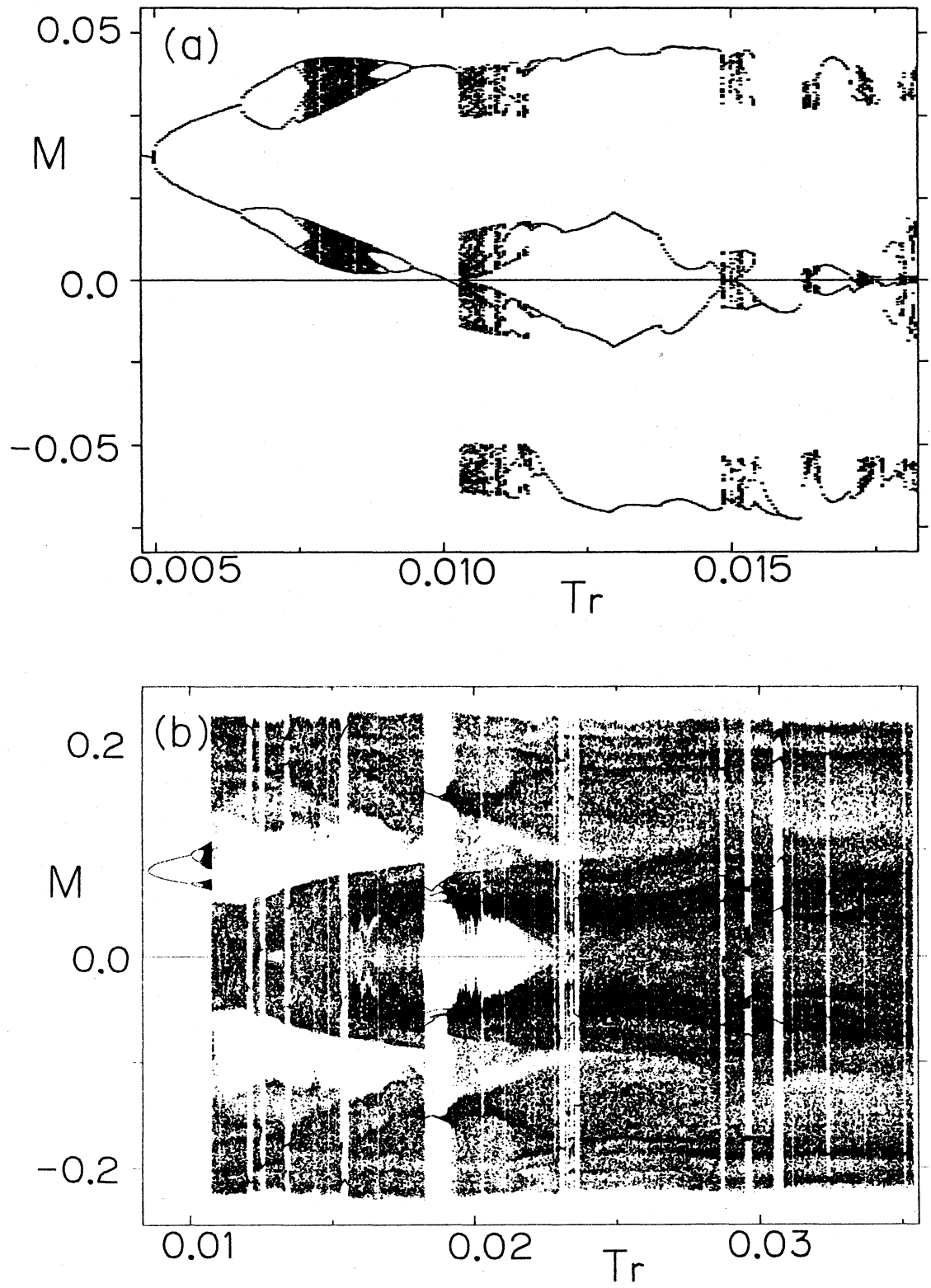


Fig.3  $T_r$ -dependence of attractors. (a)  $x_0=0.002165a$ , (b)  $0.005411a$ .

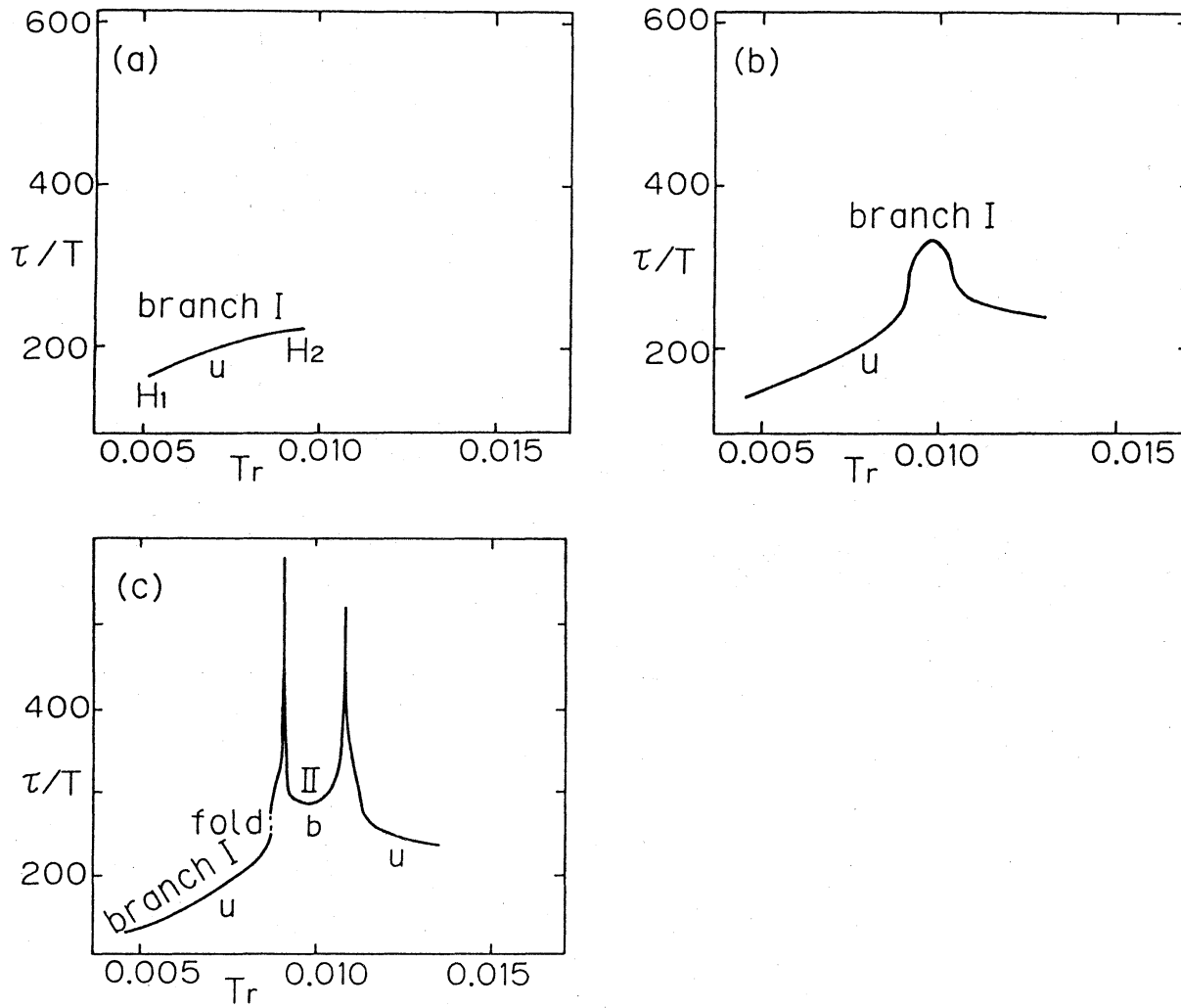


Fig.4  $T_r$ -dependence of periodic orbits. Solid and broken lines denote stable and unstable periodic orbits, respectively. u.p.o. and b.p.o. branches are expressed by  $u$  and  $b$ , respectively. (a)  $x_0/a = 0.001082$ , (b)  $0.001190$ , (c)  $0.001201$ .

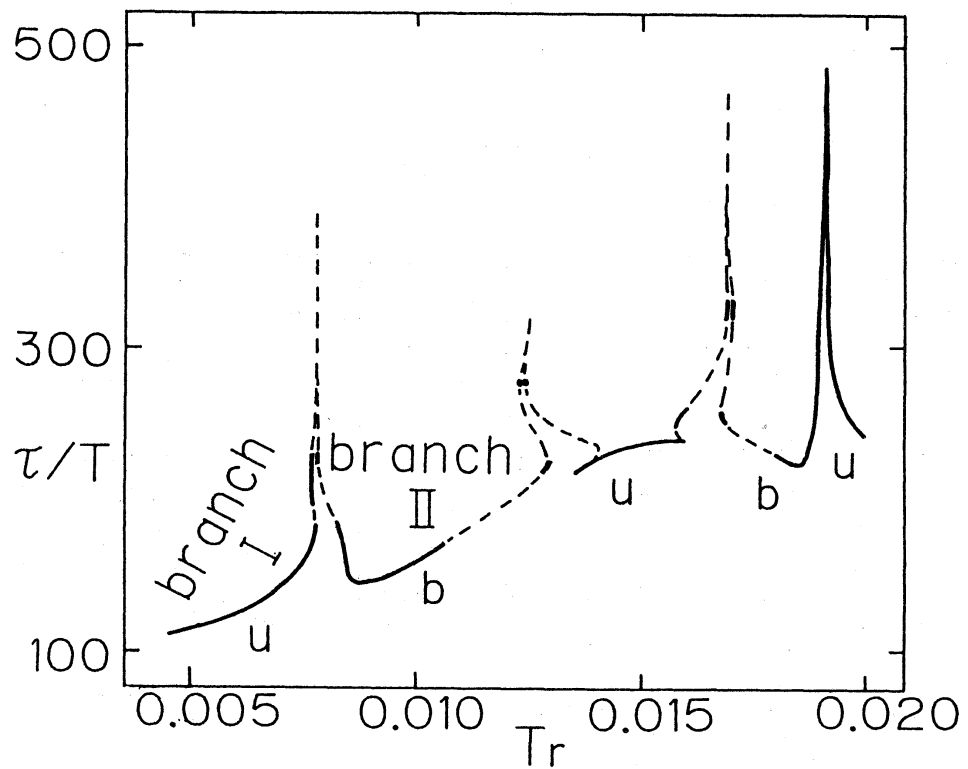


Fig.5  $T_r$ -dependence of periodic orbits. Same symbols as in Fig.4 are used.  $x_0/a = 0.001407$ .

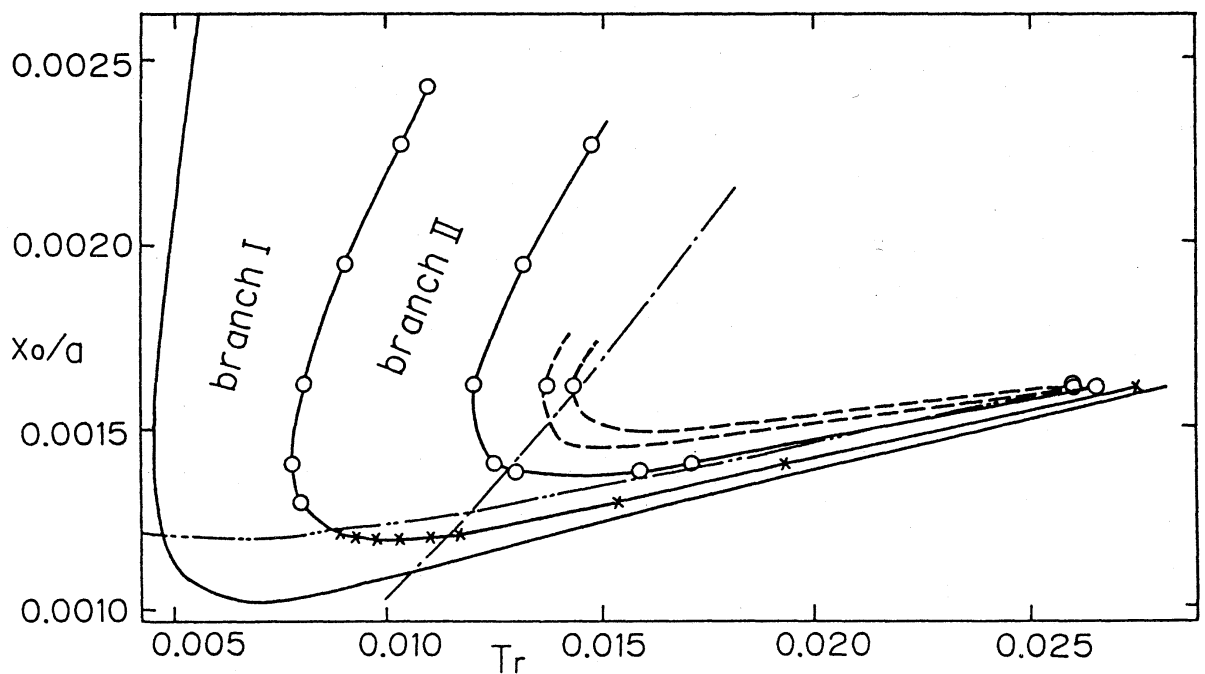


Fig.6 Parameter values for homoclinic orbits are expressed by solid lines (inferred values are shown by broken lines). Dotted-broken line denotes the turning point of the one-dimensional mode.

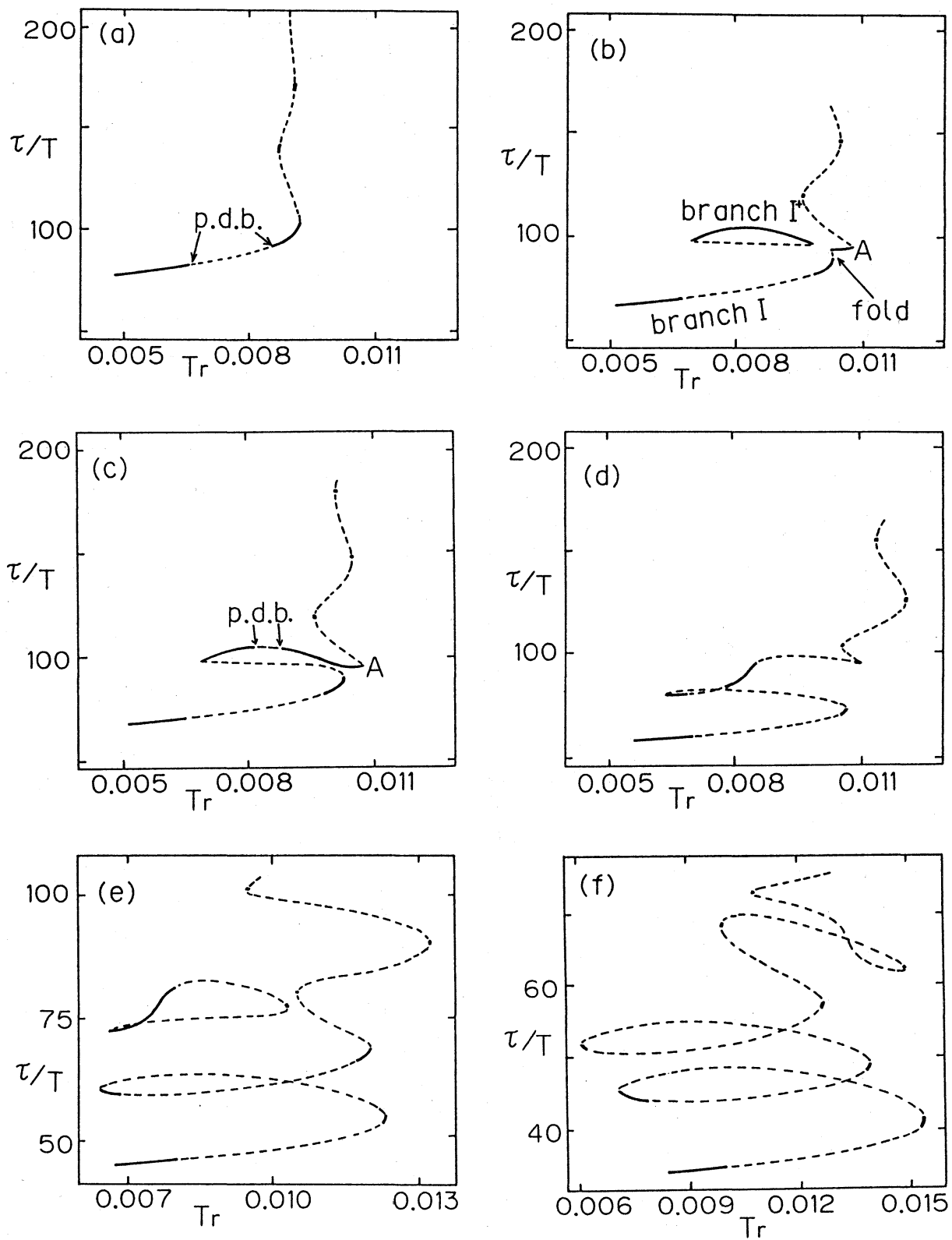


Fig.7  $T_r$ -dependence of u.p.o. of branch I. Same symbols as in Fig.4 are used. (a)  $x_0/a = 0.001948$ , (b) 0.002289, (c) 0.002294, (d) 0.002706, (e) 0.003680, (f) 0.005411.

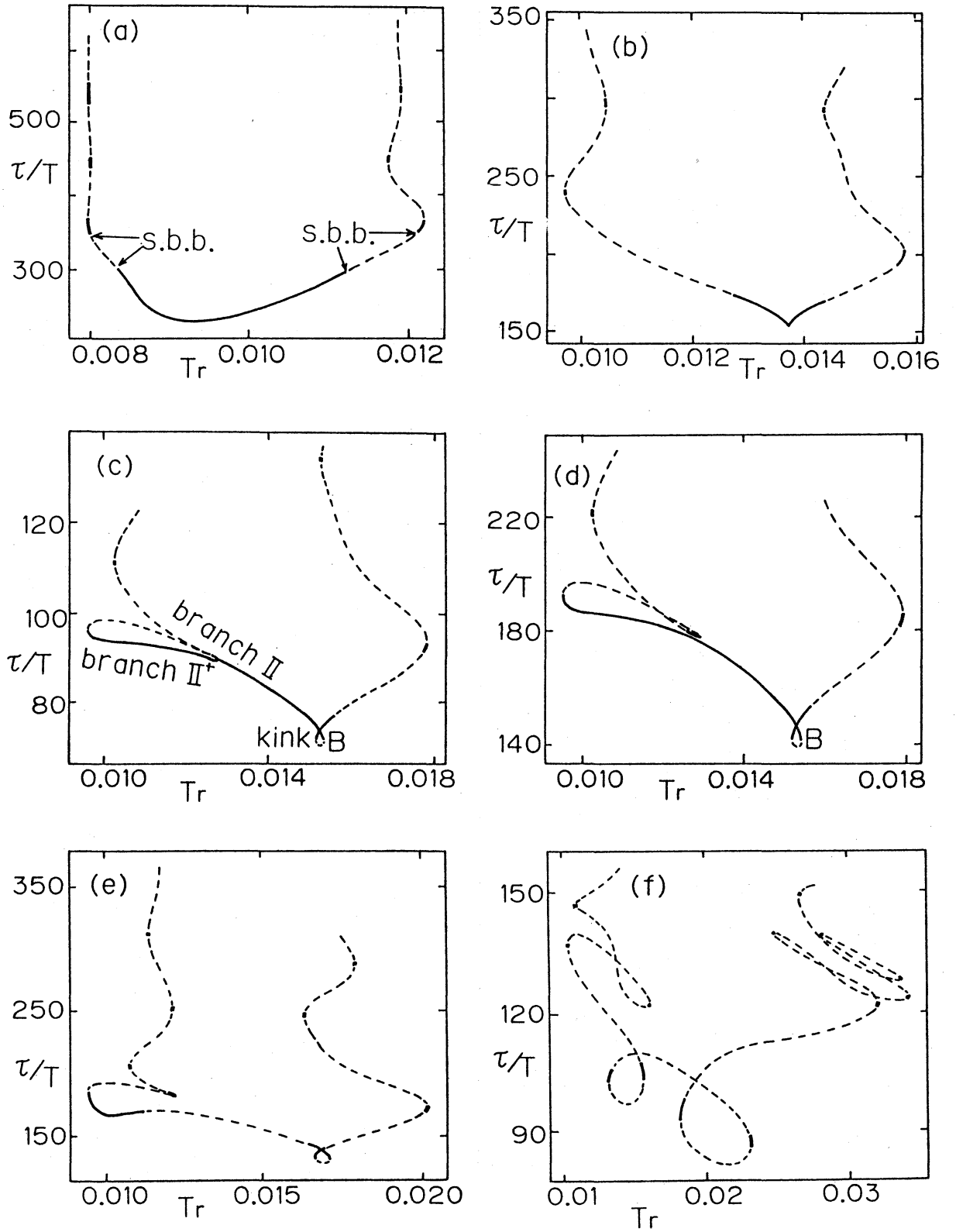


Fig.8  $T_r$ -dependence of b.p.o. of branch II. Same symbols as in Fig.4 are used. (a)  $x_0/a = 0.001623$ , (b) 0.002273, (c) 0.002478, (d) 0.002489, (e) 0.002706, (f) 0.005411.